

A Dual-level Model Predictive Control Scheme for Multi-timescale Dynamical Systems—Extended Version

Xinglong Zhang, Wei Jiang, Shuyou Yu, Xin Xu, Zhizhong Li

Abstract—So far, many control algorithms have been developed for singularly perturbed systems. However, in many industrial processes, enforcing closed-loop fast-slow dynamics for peculiarly non-separable ones is a prior request and a crucial issue to be resolved. Aiming at the above problem, this paper presents two dual-level model predictive control (MPC) algorithms for two-timescale dynamical systems with unknown bounded disturbance and input constraint. The proposed algorithms, each one composed of two regulators working in slow and fast time scales, are designed to generate closed-loop separable dynamics at the high and low levels. As a key feature, the proposed algorithms are not only suitable for singularly perturbed systems, but also capable of imposing separable closed-loop performance for dynamics that are non-separable and strongly coupled. The recursive feasibility and convergence properties are proven under suitable assumptions. The simulation results on controlling a Boiler Turbine (BT) system, including the comparisons with other classic controllers are reported, which show the effectiveness of the proposed algorithms.

Index Terms—Model predictive control, dual-level, linear systems, separable dynamics, Boiler Turbine control.

I. INTRODUCTION

Many industrial processes are characterized by separable fast-slow dynamics, which can be called “multi-timescale dynamic systems”. In a multi-timescale dynamic system, for a given constant input signal, some of the output variables reach their steady-state values fast while the other ones may experience a longer transient period, see for instance [1]–[3]. A widely-acceptable approach for the control of such systems consists in resorting to hierarchical control synthesis that possibly relies on singular perturbation theory (see the book [4]), where time-scale separation technique is adopted to define regulators at different control frequencies to guarantee the stability and

performance of the dynamics associated with the adopted channels. In addition to singularly perturbed systems, there might be systems whose dynamics are not separable but must be controlled in the same way with a multi-rate control setting, see for instance the control of a Boiler Turbine (BT) system considered in [5]. In this case, usually, the crucial controlled variables of the considered system must be adjusted at a faster rate to meet the control performance requirement, while other outputs can be controlled more smoothly in a slower time scale. As another example, the control applications for robots fit the above control problem setting. For instance, in the race car control problem, see [6], [7], the velocity is the major concern to reach the destination with minimum-time periods, while the reference tracking goal is of less importance. In urban autonomous driving applications, see [8], lane-keeping and precise tracking are the prior concerns while the velocity can be controlled in a smoother manner.

Model predictive control (MPC) is an advanced process control technique, widely used in industrial processes, such as chemical plants and smart grids, see [9]–[13], in robotics, see [14], [15], in urban traffics, see [16], and in computing data center, see [17]. In MPC, the control problem is reformulated as an optimization one, that has to be solved on-line iteratively. This allows to explicitly consider the control, state, and output constraints in the control problem. At any generic time instant k , a finite horizon optimization problem must be solved to compute the optimal control sequence. Only the first element is applied to the system, and the state and output variables are updated. The optimization problem is then repeated at the next instant $k + 1$.

In the framework of MPC, many solutions have been developed based on time-scale separation technique for systems characterized by open-loop separable dynamics. Among them, in [18] a fast-slow MPC solution has been proposed for control of nonlinear singularly perturbed systems, and the extensions to large-scale systems and to the dynamic optimization of economic cost have been addressed in [19], [20]. The algorithms utilize the reduced-order models of the original system, with model couplings between fast and slow scales disregarded, which leads to a decentralized controller design. In [21], [22], controllers designed with unitary slow or fast sampling period have been proposed for linear singularly perturbed systems with control saturation. An MPC design with closed-loop property guarantee has been presented in [23] for continuous-time singularly perturbed systems. In [24] a decentralized controller design is proposed using input-output models. In the

Xinglong Zhang, Wei Jiang, and Xin Xu are with the College of Intelligence Science and Technology, National University of Defense Technology, Changsha 410073, China. email: (zhangxinglong18@nudt.edu.cn, jiangweindt@gmail.com, xuxin_mail@263.net)

Xinglong Zhang was with the Dipartimento di Elettronica, Informazione e Bioingegneria, Politecnico di Milano, Milan 20133, Italy.

Shuyou Yu is with the State Key Laboratory of Automotive Simulation and Control and the Department of Control Science and Engineering, Jilin University at NanLing, Changchun 130025, China (e-mail: shuyou@jlu.edu.cn).

Zhizhong Li is with the State Key Laboratory of Disaster Prevention & Mitigation of Explosion & Impact, Army Engineering University, Nanjing, Jiangsu 210007, China e-mail: (lizz0607@163.com).

This work has been submitted to the IEEE for possible publication. Copyright may be transferred without notice, after which this version may no longer be accessible. The work was supported by the National Natural Science Foundation of China under Grant 61825305, 62003361, and the National Key R&D Program of China 2018YFB1305105.

application aspect, notable contributions can be found in, [25] for integrated wastewater treatment systems, [26] for control of a polymerization reactor, [27] for greenhouse climate management, and [28] for control of flexible joint manipulator. As a summary comment, almost all the aforementioned approaches are tailored for systems with clearly different dynamics due to their dependencies on singular perturbation theory, and the closed-loop stability relies on the assumption of the open-loop dynamics being separable. The control performance of such controllers could be hampered for the case that the dynamical motions are open-loop non-separable.

Motivated by the above problems, this work concerns designing dual-level algorithms based on MPC for linear multi-timescale dynamical systems with unknown bounded disturbances and input constraint, to exhibit closed-loop separable dynamic behaviors. A novel dual-level MPC (D-MPC) algorithm is initially presented for systems with bounded disturbances. The approach consists of dual levels. At the high level, an MPC problem is designed for the control commitment in the slow control channel, while a shrinking horizon MPC is designed in the basic time scale to derive satisfactory closed-loop fast dynamics. As a core contribution, an incremental form of D-MPC, i.e., *Incremental D-MPC* is proposed to improve the performance associated with the fast (crucial) output and to compensate for possible unknown piece-wise constant disturbances. Under suitable assumptions, the recursive feasibility and convergence properties of the proposed D-MPC and *Incremental D-MPC* are proven. Compared with the aforementioned works, see such as [18], [19], [23], [24], [27], the proposed ones show advantageous points in two aspects. First, the proposed ones utilize consistent models for controller designs at both time scales, being suitable for the ones with strong coupling effects that exhibit non-separable dynamics. Importantly, the controller at each time scale concerns the overall control performance in a cooperative way, which is significantly different from the decentralized independent design in the above methods.

A similar problem has been addressed in [29], however, the control scheme described in this paper shows a significant improvement for the following reasons: i) The algorithm in [29] is proposed for systems described by impulse responses, with a special focus on the viewpoint of application, while this paper presents novel solutions on the theoretical developments based on a state-space formulation, with verified closed-loop recursive feasibility and stability. ii) Due to the usage of impulse response representation, the concerned system in [29] is assumed to be strictly stable. Whereas in this paper the restriction is relaxed, i.e., the considered model is assumed stabilizable. iii) In [29], the input associated with the slow dynamics is only manipulated in the slow time scale. This could lead to control performance degradation especially for systems that are strongly coupled. To solve this problem, we allow the “slow” control variable to be refined in the fast time scale to improve the control performance.

A two-layer control structure has been proposed in [30], but the control problem considered is different. Indeed, it is designated for the coordination of large-scale independent subsystems that must produce a global constant throughput.

The approach proposed in this paper commits to enforcing separable closed-loop dynamics for strongly coupled systems and robust design under uncertainties is addressed. Hence, the control framework, and the techniques adopted in this paper are significantly different from that in [30].

The rest of the paper is organized as follows. Section 2 presents the problem description and the proposed control structure. The MPC problems at the high and low levels of the D-MPC are introduced in Section 3, while the *Incremental D-MPC* algorithm is described in Section 4. Simulation example concerning the BT control is studied in Section 5, while some conclusions are drawn in Section 6. Proofs of the theoretical results are given in the Appendix.

Notation: for a given set of variables $z_i \in \mathbb{R}^{q_i}$, $i = 1, 2, \dots, M$, we define $(z_1, z_2, \dots, z_M) = [z_1^\top \ z_2^\top \ \dots \ z_M^\top]^\top \in \mathbb{R}^q$, where $q = \sum_{i=1}^M q_i$. We use \mathbb{C} to denote the set of the complex plane. Given a matrix P , we use the symbol P^\top to denote its transpose. For a generic variable z , we denote $\Delta z(k) = z(k) - z(k-1)$, where k is the discrete-time index. We use $\|x\|_Q^2$ to represent $x^\top Q x$. We use \mathbb{N} and \mathbb{N}_+ to denote the set of non-negative and positive integers respectively. Given two sets A and B , we denote $A \times B$ as the Cartesian product. Given the signal v , we denote $\vec{v}(k : k+N-1)$ the sequence $v(k) \dots v(k+N-1)$, where N is a positive integer.

II. PROBLEM FORMULATION

The system to be controlled is described by a discrete-time linear system consisting of two interacting subsystems expressed as

$$\Sigma_s : \begin{cases} x_s(h+1) = A_{ss}x_s(h) + A_{sf}x_f(h) + B_{ss}u_s(h) + \\ \quad B_{sf}u_f(h) + d_s(h) \\ y_s(h) = C_{ss}x_s(h), \end{cases} \quad (1a)$$

$$\Sigma_f : \begin{cases} x_f(h+1) = A_{fs}x_s(h) + A_{ff}x_f(h) + B_{fs}u_s(h) + \\ \quad B_{ff}u_f(h) + d_f(h) \\ y_f(h) = C_{ff}x_f(h), \end{cases} \quad (1b)$$

where $u_s \in \mathbb{R}^{m_s}$, $x_s \in \mathbb{R}^{n_s}$, $y_s \in \mathbb{R}^{p_s}$, and $d_s \in \mathcal{D}_s \subseteq \mathbb{R}^{n_s}$ are the input, state, output variables and unmeasured disturbance belonged to Σ_s , while $u_f \in \mathbb{R}^{m_f}$, $x_f \in \mathbb{R}^{n_f}$, $y_f \in \mathbb{R}^{p_f}$, and $d_f \in \mathcal{D}_f \subseteq \mathbb{R}^{n_f}$ are the ones associated with Σ_f , \mathcal{D}_s and \mathcal{D}_f are compact sets, h is a basic discrete-time scale index, the matrices A_* , B_* (where $*$ is sf or fs in turn) represent the couplings between Σ_s and Σ_f through the state and input variables respectively.

Similar to [29], in this paper, models (1a) and (1b) are assumed to satisfy at least one of the following scenarios:

- Σ_s is characterized by a slower dynamics in contrast to Σ_f in the sense that some of the triples (u_f, x_f, y_f) reach their final steady-state values fast while the other ones, i.e. (u_s, x_s, y_s) may have begun their main dynamic motions, see the examples in [1]–[3];
- even if the dynamics of Σ_s and Σ_f might not be strictly separable, however they must be controlled in a multi-rate fashion, e.g., the triples (u_f, x_f, y_f) must react promptly

to respond to operation (reference) variations while the triples (u_s, x_s, y_s) can be controlled in a smoother fashion, see for instance [5].

Notice that, in a singularly perturbed system, couplings between different time scales are weak, hence the overall model is usually decomposed into decentralized reduced-order models with different time scales. However, in our case, interactions of the considered system can be non-separable, i.e., couplings between subsystems might be strong. To cope with possible coupling effects, system (1) can be regarded as a whole being later used in the controller design. Combining (1a), (1b), the overall system is written as

$$\Sigma: \begin{cases} x(h+1) = Ax(h) + Bu(h) + d(h) \\ y(h) = Cx(h), \end{cases} \quad (2)$$

where $u = (u_s, u_f) \in \mathbb{R}^m$, $m = m_s + m_f$, $x = (x_s, x_f) \in \mathbb{R}^n$, $n = n_s + n_f$, $y = (y_s, y_f) \in \mathbb{R}^p$, $p = p_s + p_f$, the unknown disturbance $d = (d_s, d_f) \in \mathcal{D}_s \times \mathcal{D}_f = \mathcal{D}$. The diagonal blocks of the collective state transition matrix A and input matrix B are A_{ss} , A_{ff} and B_{ss} , B_{ff} respectively; whereas their non-diagonal blocks correspond to the coupling terms of the state and input variables between Σ_s and Σ_f . The collective output matrix is $C = \text{diag}(C_{ss}, C_{ff})$.

The control objectives to be achieved are introduced here.

- (i) **Setpoint regulation:** for a given reference value $y_r = (y_{s,r}, y_{f,r})$, we aim to drive

$$y_s(h) \rightarrow y_{s,r}, \quad (3a)$$

$$y_f(h) \rightarrow y_{f,r} \quad (3b)$$

- (ii) **Input constraint:** enforce the input constraint of the type

$$u_s(h) \in \mathcal{U}_s, \quad (4a)$$

$$u_f(h) \in \mathcal{U}_f, \quad (4b)$$

where $\mathcal{U}_s, \mathcal{U}_f$ are convex sets, $\mathcal{U} = \mathcal{U}_s \times \mathcal{U}_f$.

The following assumption is assumed to hold:

Assumption 1:

- (1) The pair (A, B) is stabilizable;
- (2) $m_f = p_f$. Also, a steady-state pair (u_r, x_r) exists associated with the reference y_r , such that $x_r = Ax_r + Bu_r$, $y_r = Cx_r$, $x_r = (x_{s,r}, x_{f,r})$, and $u_r = (u_{s,r}, u_{f,r}) \in \mathcal{U}_s \times \mathcal{U}_f$.

Remark 1: Assumption 1.(2) allows the considered system (2) being non-square, i.e., $m_s \neq p_s$. Specifically, for $m \leq p$, given reachable setpoint y_r , one can compute $(x_r, u_r) = \Phi^\dagger(0, y_r)$, where

$$\Phi = \begin{bmatrix} I - A & -B \\ C & 0 \end{bmatrix},$$

$\Phi^\dagger = (\Phi^\top \Phi)^{-1} \Phi$. For $p < m$, multiple steady-state solutions might exist associated with y_r . In this case, one can select a suitable steady-state pair via solving a static optimization problem with respect to the decision variable x, u , optimizing a user-specified economic performance index subject to the constraints $x = Ax + Bu$, $y_r = Cx$, $u \in \mathcal{U}$.

In principle, a centralized MPC problem with respect to Σ can be solved so as to achieve the above objectives. However,

the resulting control performance might be hampered in the aforementioned scenarios due to the conflicting requirements of the sampling period and prediction horizon for Σ_s and Σ_f respectively.

For this reason, a dual-level MPC (D-MPC) is initially proposed in this paper to fulfill the aforementioned control objectives. As shown in Figure 1, at the high level, a slow time scale k associated with $N \in \mathbb{N}$ period of the basic time scale h is adopted to define an MPC problem concerning the sampled version of Σ . The computed values of the control actions at this level, $u_f^{[N]}(k)$, $u_s^{[N]}(k)$, are held constant within the long sampling time interval $[kN, kN + N)$, i.e., $\bar{u}_f(h) = u_f^{[N]}(k)$, $\bar{u}_s(h) = u_s^{[N]}(k)$ for all $h \in [kN, kN + N)$. At the low level, a shrinking horizon MPC is designed at the basic time scale to refine control actions with additional corrections (i.e., $\delta u_f(h)$, $\delta u_s(h)$) in order to derive satisfactory short-term transient associated with the closed-loop fast dynamics and to account for possible disturbances.

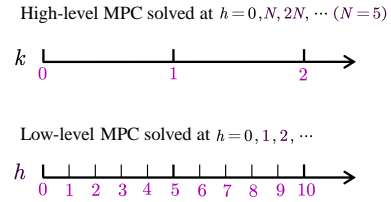


Fig. 1. The time indices adopted in different levels: $h = 1, 2, \dots$ denotes the basic (fast) time instant, while $h = 0, N, 2N, \dots$ denotes the slow time instant in the basic time scale. The above figure shows a special case with $N = 5$.

The overall control actions of the D-MPC regulator are described by

$$u_s(h) = \bar{u}_s(h) + \delta u_s(h), \quad (5a)$$

$$u_f(h) = \bar{u}_f(h) + \delta u_f(h) \quad (5b)$$

where

- the control actions $\bar{u}_s(h)$ and $\bar{u}_f(h)$ will be computed by solving an MPC problem according to receding horizon principle in the slow time scale to fulfill objective (3a) and (4a), (4b);
- the corrections $\delta u_s(h)$ and $\delta u_f(h)$ will be defined by a shrinking horizon MPC regulator running in the basic time scale to fulfill objective (3b) and to enforce constraints (4a), (4b).

Moreover, to further improve the control behavior of the fast controlled variables, an *Incremental D-MPC* algorithm is also proposed (see Section IV). To be specific, this version includes integral actions at the two levels and, a prior explicit design of the output trajectory of y_f at the slow time scale to enforce y_f to the reference value or its neighbor promptly. A brief diagram of the proposed approaches is displayed in Figure 2.

III. D-MPC ALGORITHM

In this section, the D-MPC algorithm consisting of an MPC at the high level and a shrinking horizon MPC at the low level is devised.

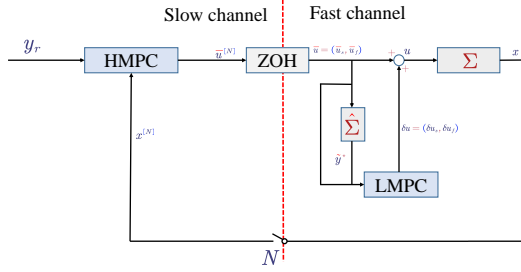


Fig. 2. A brief diagram of the proposed control scheme: HMPC (LMPC) stands for the MPC at the higher (lower) level, while ZOH is the zero order holder.

A. MPC at the high level

In order to design the high-level regulator in the slow time scale k (see again Figure 1), denote by $u_*^{[N]}$, $x_*^{[N]}$, $y_*^{[N]}$, and $d_*^{[N]}$ the samplings of u_* , x_* , y_* , and d_* (where $*$ is s or f , in turn) and by $u^{[N]} = (u_s^{[N]}, u_f^{[N]})$, $x^{[N]} = (x_s^{[N]}, x_f^{[N]})$, $y^{[N]} = (y_s^{[N]}, y_f^{[N]})$, and $d^{[N]} = (d_s^{[N]}, d_f^{[N]})$ the samplings of the input, state, and output variables corresponding to the time scale k . Hence, the sampled version of (2) with N period is given as

$$\Sigma^{[N]} : \begin{cases} x^{[N]}(k+1) = A^{[N]}x^{[N]}(k) + B^{[N]}u^{[N]}(k) + \tilde{d}^{[N]}(k) \\ y^{[N]}(k) = Cx^{[N]}(k), \end{cases} \quad (6)$$

where $A^{[N]} = A^N$, $B^{[N]} = \sum_{j=0}^{N-1} A^{N-j-1}B$, $\tilde{d}^{[N]}(k) = f_{\delta u}^{[N]}(k) + d^{[N]}(k)$, $d^{[N]}(k) = \sum_{i=0}^{N-1} A^i d(kN+i)$, $f_{\delta u}^{[N]}(k) = \sum_{i=0}^{N-1} A^i B \delta u(kN+i)$ is due to the control at the low level.

The following proposition can be stated for $\Sigma^{[N]}$:

Proposition 1: The pair $(A^{[N]}, C)$ is detectable if (A, C) is detectable.

Also, the following assumption about $\Sigma^{[N]}$ is assumed to be holding:

Assumption 2: The pair $(A^{[N]}, B^{[N]})$ is stabilizable.

Remark 2: Note that, slightly different from the detectability condition in Proposition 1, to meet the stabilizability requirement of $\Sigma^{[N]}$, we require Assumption 2 to be verified a posteriori once the sampling period N is chosen. This is due to the fact that, starting from the stabilizability of (A, B) , there is no guarantee the resultant sampled pair $(A^{[N]}, B^{[N]})$ is also stabilizable. A simple example to illustrate this point is as follows: consider a single-input single-output system described by $x(h+1) = -x(h) + u(h)$, which is obviously stabilizable. However, the $N = 2$ period sampled version $x^{[2]}(k+1) = (-1)^2 x^{[2]}(k) + (-1+1)u^{[2]}(k) = x^{[2]}(k)$ is not stabilizable.

As the disturbance term $\tilde{d}^{[N]}$ is unknown, for prediction, we introduce the following nominal model:

$$\hat{\Sigma}^{[N]} : \begin{cases} \hat{x}^{[N]}(k+1) = A^{[N]}\hat{x}^{[N]}(k) + B^{[N]}u^{[N]}(k) \\ \hat{y}^{[N]}(k) = C\hat{x}^{[N]}(k), \end{cases} \quad (7)$$

Notice that, if $\hat{x}(kN) = \hat{x}^{[N]}(k)$ and the control $u(h) = u^{[N]}(k)$, $\forall h \in [kN, kN+N)$, it holds that $\hat{x}(kN+N) = \hat{x}^{[N]}(k+1)$ and $\hat{y}(kN+N) = \hat{y}^{[N]}(k+1)$.

With (7), it is now possible to state the MPC problem at the

high level. At each slow time-step k we solve an optimization problem according to receding horizon principle as follows:

$$\min_{\bar{u}^{[N]}(k:k+N_H-1)} J_H \quad (8)$$

where

$$J_H = \sum_{i=0}^{N_H-1} (\|\hat{y}^{[N]}(k+i) - y_r\|_{Q_H}^2 + \|u^{[N]}(k+i) - u_r\|_{R_H}^2) + \|\hat{x}^{[N]}(k+N_H) - x_r\|_{P_H}^2, \quad (9)$$

and where $N_H > 0$ is the adopted prediction horizon. The parameters $Q_H \in \mathbb{R}^{p \times p}$, $R_H \in \mathbb{R}^{m \times m}$ are positive definite and symmetric weighting matrices, while $P_H \in \mathbb{R}^{n \times n}$ is computed as the solution to the Lyapunov equation described by

$$F_H^\top P_H F_H - P_H = -(C^\top Q_H C + K_H^\top R_H K_H) \quad (10)$$

where matrix $F_H = A^{[N]} + B^{[N]}K_H$ is Schur stable and K_H is a stabilizing gain matrix.

The optimization problem (8) is performed under the following constraints:

- (1) the dynamics (7);
- (2) the input constraint

$$u^{[N]}(k+i) \in \bar{\mathcal{U}},$$

where $\bar{\mathcal{U}}$ is a tightened convex set of \mathcal{U} , i.e., $\bar{\mathcal{U}} \subseteq \mathcal{U}$;

- (3) the terminal state constraint

$$\hat{x}^{[N]}(k+N_H) \in \mathcal{X}_F^s,$$

where $\mathcal{X}_F^s \subseteq \mathcal{X}_F$, the set \mathcal{X}_F is chosen as a positively invariant set for system (7) controlled with the stabilizing control law $u^{[N]}(k) = K_H(\hat{x}^{[N]}(k) - x_r) + u_r$, satisfying $K_H(\mathcal{X}_F \ominus x_r) \subseteq \mathcal{U} \ominus u_r$. To guarantee the recursive feasibility under uncertainties, \mathcal{X}_F^s is selected such that: for any $z(k) \in \mathcal{X}_F$, the successive state under the above stabilizing control law satisfies $z(k+1) \in \mathcal{X}_F^s$. Let $\bar{u}^{[N]}(k:k+N_H-1|k)$ be the optimal solution to optimization (8). Only the first element $u^{[N]}(k|k)$ is used for designing the regulator at the low level that will be applied in the fast time scale. At the next time $k+1$, the optimization is repeated according to receding horizon principle.

B. Shrinking horizon MPC at the low level

Assume now to be at a specific basic time instant $h = kN$ (correspond to the slow time instant k , see Figure 1) such that the high-level optimization problem (8) with cost (9) has been successfully solved. Thus the computed values of the input $u^{[N]}(k) = (u_s^{[N]}(k), u_f^{[N]}(k))$ and the one-step ahead state prediction $\hat{x}^{[N]}(k+1|k)$ are available. Let us focus on the output performance in the fast time scale within the interval $h \in [kN, kN+N)$. Denoting by $\tilde{y}(h) = (\tilde{y}_s(h), \tilde{y}_f(h))$ the output resulting from (7) with $u(h) = u^{[N]}(\lfloor h/N \rfloor)$, the component $\tilde{y}_f(h)$ may expect undesired transient due to the use of the long sampling period at the high level.

For this reason, at the low level the overall control action associated with y_f is refined as

$$u_f(h) = \bar{u}_f(h) + \delta u_f(h) \quad (11a)$$

where $\bar{u}_f(h) = u_f^{[M]}(\lfloor h/N \rfloor)$, δu_f is computed at the low level by a properly defined optimization problem, which is deferred in (13).

Since $\delta u_f(h)$ could influence the value of $y_s(h)$ in the fast time scale due to possible nonzero coupling terms from Σ_f to Σ_s (e.g. A_{sf} , B_{sf}), it is also convenient to allow a further control freedom of u_s leading to the correction as follows:

$$u_s(h) = \bar{u}_s(h) + \delta u_s(h) \quad (11b)$$

where $\bar{u}_s(h) = u_s^{[M]}(\lfloor h/N \rfloor)$, δu_s is another decision variable at the low level.

In view of (11), one can rewrite (2) with $u(h) = \bar{u}(h) + \delta u(h)$, where $\bar{u} = (\bar{u}_s, \bar{u}_f)$, $\delta u = (\delta u_s, \delta u_f)$. However, for prediction purpose, we define a prediction model by neglecting the effect of d :

$$\hat{\Sigma}: \begin{cases} \hat{x}(h+i+1|h) = A\hat{x}(h+i|h) + Bu(h+i|h) \\ \hat{y}(h+i|h) = C\hat{x}(h+i|h) \end{cases} \quad (12)$$

where $\hat{x}(h|h) = x(h)$. Accordingly, at any fast time instant $h = kN + t$, letting $\vec{\delta u}(h : (k+1)N - 1) = [\delta u(h|h) \cdots \delta u((k+1)N - 1|h)] \in (\mathbb{R}^m)^{N-t}$, a shrinking horizon MPC problem can be solved at the low level:

$$\min_{\vec{\delta u}(h:(k+1)N-1)} J_L \quad (13)$$

where

$$J_L = \sum_{j=0}^{N-t-1} \|\hat{y}(h+j|h) - \bar{y}^*(h)\|_Q^2 + \|\delta u(h+j|h)\|_R^2 \quad (14)$$

and where $\bar{y}^*(h) = (\bar{y}_s(h), \bar{y}_f(kN+N))$, $h \in [kN, kN+N)$, \bar{y}_s and \bar{y}_f are defined above (11b).

The optimization problem (13) is performed under the following constraints:

- (1) the dynamics (12);
- (2) the input constraint

$$\begin{aligned} u^{[M]}(\lfloor h/N \rfloor) + \delta u(h|h) &\in \mathcal{U}, \\ u^{[M]}(\lfloor h/N \rfloor) + \delta u(h+j|h) &\in \hat{\mathcal{U}}^i, \quad \forall j = 1, \dots, N-t-1, \end{aligned} \quad (15)$$

where $\hat{\mathcal{U}}^i$ is such that $\bar{\mathcal{U}} \subseteq \hat{\mathcal{U}}^i \subseteq \mathcal{U}$, $i = h - kN$;

- (3) the state terminal constraint

$$\hat{x}(kN+N|h) = \hat{x}^{[M]}(k+1|k). \quad (16)$$

Remark 3: The rationale of choosing signal $\bar{y}^*(h)$ as the reference for the low level lies in the fact that $\hat{y}_f(h)$ is expected to react promptly to respond to $\bar{y}_f(kN+N)$, while $\hat{y}_s(h)$ can be controlled to follow the smooth trajectory $\bar{y}_s(h)$ generated from the high level.

Remark 4: It is highlighted that the structure of the proposed approach is different from that of the cascade ones, see for instance [31], for the reason that in the cascade algorithm, the computed input from the high level is considered as the output reference to be tracked at the low level, while the proposed algorithms utilize the control action computed from the high level, i.e., $\bar{u}(h)$, to generate the possible reference profile with model (2) in an open-loop fashion.

C. Summary of the D-MPC algorithm

In summary, the main steps for the on-line implementation of the D-MPC are given in Algorithm 1.

Algorithm 1 On-line implementation of D-MPC

initialization

while for any integer $k \geq 0$ **do**

h1) compute the control $u^{[M]}(k|k)$ by solving the optimization problem (8) with (9) and update $\hat{x}^{[M]}(k+1|k)$

h2) generate the open-loop output $\bar{y}^*(h)$ from (2) with $u(h) = u^{[M]}(\lfloor h/N \rfloor)$, for all $h \in [kN, kN+N)$

for $h \leftarrow kN$ **to** $kN+N-1$ **do**

11) compute $\delta u(h|h)$ with optimization problem (13) with (14) and apply $u(h) = u^{[M]}(\lfloor h/N \rfloor) + \delta u(h|h)$ to (2)

12) update $x(h+1)$, $y(h+1)$, set $\hat{x}(h+1) = x(h+1)$, $\hat{y}(h+1) = y(h+1)$

end

h3) $k \leftarrow k+1$

end

Theorem 1: Under Assumption 1, if the initial condition is such that $\hat{x}^{[M]}(0) = \hat{x}(0) = x(0)$ and (8) is feasible at $k=0$, then the following results can be stated for the proposed D-MPC control algorithm.

- (1) Provided that

$$(A^{[M]})^{N_H-1} \mathcal{D} \subseteq \mathcal{X}_F \ominus \mathcal{X}_F^s \quad (17)$$

and at any time $h \in [kN, kN+N-2]$ that,

$$-A^{N-j-1} \mathcal{D} \oplus L^j \hat{\mathcal{U}}^j \subseteq \Delta L^j \mathcal{U} \oplus L^{j+1} \hat{\mathcal{U}}^{j+1} \quad (18)$$

where $L^j = \sum_{i=j+1}^{N-1} A^{N-i-1} B$, $\Delta L^j = L^j - L^{j+1}$, $j = h - kN$, then the feasibility can be guaranteed:

- for the high-level problem (8) at all slow time instant $k > 0$;
 - for the low-level problem (13) at all fast time instant $h \geq 0$.
- (2) If the disturbance $d = 0$, then the asymptotic convergence of the closed-loop system can be ensured:

- The slow-time scale system $\Sigma^{[M]}$ enjoys the convergence property, i.e., $\lim_{k \rightarrow +\infty} (u^{[M]}(k), x^{[M]}(k), y^{[M]}(k)) = (u_r, x_r, y_r)$.
- Moreover, for the low-level problem (13), it holds that $\lim_{h \rightarrow +\infty} \delta u(h) = 0$. Finally, $\lim_{h \rightarrow +\infty} (u(h), x(h), y(h)) = (u_r, x_r, y_r)$.

Note that, the terminal constraint (16) plays a crucial role for guaranteeing the closed-loop properties of the D-MPC. However, as the proposed D-MPC control structure is an upper-bottom one, the computed value of $\hat{x}_f^{[M]}(k)$ at the high level influences the control performance at the low level due to (16). For this reason, the state $\hat{x}_f(h)$ associated with $\hat{y}_f(h)$ in the basic time scale might not converge to its nominal value faster than $\hat{x}_s(h)$ especially for systems that exhibit nonseparable open-loop dynamics. We solve this problem in the following section.

IV. Incremental D-MPC ALGORITHM

In this section, we design an *Incremental D-MPC* algorithm to improve the control performance associated with the ‘‘fast’’ output y_f and to compensate for possible time-varying piecewise constant or smooth uncertainties.

A. Design of the Incremental D-MPC

In the following we first focus on the re-design of the MPC regulator at the high level. To this end, we first partition the above sampled system as the one with the structure similar to (1). To proceed, we rewrite the matrices $A^{[N]}$, $B^{[N]}$, and vector $\tilde{d}^{[N]}$ into the following forms

$$A^{[N]} = \begin{bmatrix} A_{ss}^{[N]} & A_{sf}^{[N]} \\ A_{fs}^{[N]} & A_{ff}^{[N]} \end{bmatrix}, \quad B^{[N]} = \begin{bmatrix} B_{ss}^{[N]} & B_{sf}^{[N]} \\ B_{fs}^{[N]} & B_{ff}^{[N]} \end{bmatrix}, \quad \tilde{d}^{[N]} = \begin{bmatrix} \tilde{d}_s^{[N]} \\ \tilde{d}_f^{[N]} \end{bmatrix}$$

where $A_{ss}^{[N]} \in \mathbb{R}^{n_s \times n_s}$, $B_{ss}^{[N]} \in \mathbb{R}^{n_s \times m_s}$, $\tilde{d}_s^{[N]} \in \mathbb{R}^{n_s}$.

In view of this, the sampled perturbed system (6) can be partitioned as two interacting ones as follows:

$$\Sigma_s^{[N]} : \begin{cases} x_s^{[N]}(k+1) = A_{ss}^{[N]}x_s^{[N]}(k) + A_{sf}^{[N]}x_f^{[N]}(k) + B_{ss}^{[N]}u_s^{[N]}(k) \\ \quad + B_{sf}^{[N]}u_f^{[N]}(k) + \tilde{d}_s^{[N]}(k) \\ y_s^{[N]}(k) = C_{ss}x_s^{[N]}(k), \end{cases} \quad (19a)$$

$$\Sigma_f^{[N]} : \begin{cases} x_f^{[N]}(k+1) = A_{fs}^{[N]}x_s^{[N]}(k) + A_{ff}^{[N]}x_f^{[N]}(k) + B_{fs}^{[N]}u_s^{[N]}(k) \\ \quad + B_{ff}^{[N]}u_f^{[N]}(k) + \tilde{d}_f^{[N]}(k) \\ y_f^{[N]}(k) = C_{ff}x_f^{[N]}(k), \end{cases} \quad (19b)$$

The following assumption about $\Sigma_f^{[N]}$ is assumed to hold:

Assumption 3: Matrix $C_{ff}B_{ff}^{[N]}$ is full rank.

With (19), with the goal of guaranteeing satisfactory control performance related to y_f in the basic time scale, it is convenient to enforce all the future predictions $y_f^{[N]}(k)$, $\forall k > 0$ associated with $\Sigma_f^{[N]}$ being equal to the reference value $y_{f,r}$. In this way, the real output y_f resulting from controller (13) will reach the reference $y_{f,r}$ in only one slow-time step. However, this restriction might cause infeasibility issue in case $y_{f,r}$ is far from its initial value $y_f(0)$, and/or constraints on the control increments are enforced. For this reason, instead of imposing $y_f^{[N]}(k) = y_{f,r} \forall k > 0$, one can enforce the following relation

$$y_f^{[N]}(k) = \tilde{y}_{f,r}(k) \quad \forall k > 0, \quad (20)$$

where $\tilde{y}_{f,r}(k) = y_f(0) + \alpha(k)(y_{f,r} - y_f(0))$ and where $\alpha(k)$ is defined as an optimization variable that its value is restricted by $0 \leq \alpha(k) \leq 1$ and reaches 1 in finite time steps, i.e.,

$$\begin{cases} \alpha(0) = 0, \\ 0 \leq \alpha(k) \leq 1, \quad k \in [1, N_\alpha] \\ \alpha(k) = 1, \quad k \geq N_\alpha \end{cases} \quad (21)$$

where N_α is a positive integer. As $\tilde{d}_f^{[N]}(k)$ is unknown at time k , (20) can be slightly relaxed, i.e., we enforce at time k $\hat{y}_f^{[N]}(k+j) = \tilde{y}_{f,r}(k+j)$. In view of (19), it is required that

$$u_f^{[N]}(k+j) = (C_{ff}B_{ff}^{[N]})^{-1}(\tilde{y}_{f,r}(k+j) - C_{ff}\left[\begin{matrix} A_{fs}^{[N]} & A_{ff}^{[N]} \end{matrix}\right]\hat{x}^{[N]}(k+j) + B_{fs}^{[N]}u_s^{[N]}(k+j)) \quad (22)$$

where \hat{x} is the predicted value of x . Under constraint (22), the time steps required for $\hat{y}_f^{[N]} = y_{f,r}$ can be defined via properly tuning parameter N_α .

By substituting $u_f^{[N]}$ with (22), one can write the one-step ahead state prediction at time k , i.e.,

$$\begin{cases} \hat{x}^{[N]}(k+1) = \tilde{A}^{[N]}\hat{x}^{[N]}(k) + \tilde{B}_s^{[N]}u_s^{[N]}(k) + \tilde{B}_f^{[N]}\tilde{y}_{f,r}(k) \\ \hat{y}_s^{[N]}(k) = \tilde{C}_s\hat{x}^{[N]}(k), \end{cases} \quad (23)$$

$$\text{where } \hat{x}^{[N]}(k) = x^{[N]}(k), \quad \tilde{A}^{[N]} = \begin{bmatrix} \tilde{A}_{ss}^{[N]} & \tilde{A}_{sf}^{[N]} \\ \tilde{A}_{fs}^{[N]} & \tilde{A}_{ff}^{[N]} \end{bmatrix}, \quad \tilde{B}_s^{[N]} = \begin{bmatrix} \tilde{B}_{ss}^{[N]} \\ \tilde{B}_{fs}^{[N]} \end{bmatrix},$$

$$\tilde{B}_f^{[N]} = \begin{bmatrix} \tilde{B}_{sf}^{[N]} \\ \tilde{B}_{ff}^{[N]} \end{bmatrix}, \quad \tilde{C}_s = \begin{bmatrix} C_{ss} \\ 0 \end{bmatrix}^\top, \quad \text{and where}$$

$$\begin{aligned} \tilde{A}_{ss}^{[N]} &= A_{ss}^{[N]} - B_{sf}^{[N]}(C_{ff}B_{ff}^{[N]})^{-1}C_{ff}A_{fs}^{[N]} \\ \tilde{A}_{sf}^{[N]} &= A_{sf}^{[N]} - B_{sf}^{[N]}(C_{ff}B_{ff}^{[N]})^{-1}C_{ff}A_{ff}^{[N]} \\ \tilde{A}_{fs}^{[N]} &= A_{fs}^{[N]} - B_{ff}^{[N]}(C_{ff}B_{ff}^{[N]})^{-1}C_{ff}A_{fs}^{[N]} \\ \tilde{A}_{ff}^{[N]} &= A_{ff}^{[N]} - B_{ff}^{[N]}(C_{ff}B_{ff}^{[N]})^{-1}C_{ff}A_{ff}^{[N]} \\ \tilde{B}_{ss}^{[N]} &= B_{ss}^{[N]} - B_{sf}^{[N]}(C_{ff}B_{ff}^{[N]})^{-1}C_{ff}B_{fs}^{[N]} \\ \tilde{B}_{fs}^{[N]} &= B_{fs}^{[N]} - B_{ff}^{[N]}(C_{ff}B_{ff}^{[N]})^{-1}C_{ff}B_{fs}^{[N]} \\ \tilde{B}_{sf}^{[N]} &= B_{sf}^{[N]}(C_{ff}B_{ff}^{[N]})^{-1} \\ \tilde{B}_{ff}^{[N]} &= B_{ff}^{[N]}(C_{ff}B_{ff}^{[N]})^{-1}. \end{aligned}$$

Assumption 4: The integer N is such that $\tilde{A}^{[N]}$ is stabilizable. To account for the model uncertainties, model (23) is reformulated in the *incremental form* and used for defining an MPC including an integral action. In doing so, the closed-loop system is capable to compensate for the influences caused by smoothly varying disturbances, see [32]. To this end, letting $\tilde{x}^{[N]}(k) = (\hat{y}_s^{[N]}(k), \Delta\hat{x}^{[N]}(k))$, from (23) we compute

$$\begin{cases} \tilde{x}^{[N]}(k+1) = \tilde{A}^{[N]}\tilde{x}^{[N]}(k) + \tilde{B}_s^{[N]}\Delta u_s^{[N]}(k) + \tilde{B}_f^{[N]}\Delta\alpha(k)(y_{f,r} - y_f(0)) \\ \alpha(k) = \alpha(k-1) + \Delta\alpha(k) \\ \hat{y}_s^{[N]}(k) = \tilde{C}\tilde{x}^{[N]}(k), \end{cases} \quad (24)$$

where $\tilde{A}^{[N]} = \begin{bmatrix} I & \tilde{C}_s\tilde{A}^{[N]} \\ 0 & \tilde{A}^{[N]} \end{bmatrix}$, $\tilde{B}_s^{[N]} = \begin{bmatrix} \tilde{C}_s\tilde{B}_s^{[N]} \\ \tilde{B}_s^{[N]} \end{bmatrix}$, $\tilde{B}_f^{[N]} = \begin{bmatrix} \tilde{C}_s\tilde{B}_f^{[N]} \\ \tilde{B}_f^{[N]} \end{bmatrix}$, $\tilde{C} = \begin{bmatrix} I & 0 \end{bmatrix}$.

Proposition 2: The pair $(\tilde{A}^{[N]}, \tilde{B}_s^{[N]})$ is stabilizable if and only if

$$\begin{aligned} &\bullet \text{rank}\left(\begin{bmatrix} \tilde{C}_s\tilde{A}^{[N]} & \tilde{C}_s\tilde{B}_s^{[N]} \\ \tilde{A}^{[N]} - I & \tilde{B}_s^{[N]} \end{bmatrix}^\top\right) = n + p_s, \\ &\bullet \text{rank}\left(\begin{bmatrix} 2I & 0 \\ \tilde{C}_s\tilde{A}^{[N]} & \tilde{A}^{[N]} + I \\ \tilde{C}_s\tilde{B}_s^{[N]} & \tilde{B}_s^{[N]} \end{bmatrix}^\top\right) = n + p_s. \end{aligned}$$

Under proposition 2, it is possible to find a gain matrix $\tilde{K}_{s,H}$ such that $\tilde{F}_{s,H} = \tilde{A}^{[N]} + \tilde{B}_s^{[N]}\tilde{K}_{s,H}$ is Schur stable.

Note that, it is not straightforward to write the constraints on $\tilde{u}_s^{[N]}$ and $\tilde{u}_f^{[N]}$ using model (24). We are going to show that, in

line with [32], it is possible to represent the control variables by the state in the *incremental form*, i.e.,

$$\begin{aligned}\bar{u}_s^{[M]}(k) &= \Gamma_{us}(\bar{x}^{[M]}(k+1) - \bar{B}_f^{[M]}\bar{y}_{f,r}) \\ \bar{u}_f^{[M]}(k) &= (C_{ff}B_{ff}^{[M]})^{-1}(\bar{y}_{f,r}(k) - \\ &\quad \Gamma_{uf}(\bar{x}^{[M]}(k+1) - \bar{B}_f^{[M]}\bar{y}_{f,r}))\end{aligned}\quad (25)$$

where $\Gamma_{uf} = C_{ff} \begin{bmatrix} A_{fs}^{[M]} & A_{ff}^{[M]} & B_{fs}^{[M]} \end{bmatrix} \Gamma$, $\Gamma_{us} = [0_n \quad I_{m_s}] \Gamma$, and

$$\text{where } \Gamma = \begin{bmatrix} \bar{C}_s \bar{A}^{[M]} & \bar{C}_s \bar{B}_s^{[M]} \\ \bar{A}^{[M]} - I_n & \bar{B}_s^{[M]} \end{bmatrix}^{-1}.$$

In view of (4a), (4b), (25), to enforce constraints on $(\bar{u}_s^{[M]}(k), \bar{u}_f^{[M]}(k)) \in \mathcal{U}_s \times \mathcal{U}_f$, one can use

$$A_x \bar{x}^{[M]}(k+1) + b_y \in \bar{\mathcal{U}} \quad (26)$$

where $A_x = \begin{bmatrix} \Gamma_{us}^\top & -\Gamma_{uf}^\top \end{bmatrix}^\top$, $b_y = \begin{bmatrix} -(\Gamma_{us} \bar{B}_f^{[M]})^\top & (C_{ff} B_{ff}^{[M]})^{-\top} + ((C_{ff} B_{ff}^{[M]})^{-1} \Gamma_{uf} \bar{B}_f^{[M]})^\top \end{bmatrix}^\top \bar{y}_{f,r}$.

Based on (24) and (26), now we state the *Incremental MPC* problem at the high level. At each slow time-step k we solve an optimization problem according to receding horizon principle as follows:

$$\min_{\bar{\Delta u}_s^{[M]}(k:k+\bar{N}_H-1)} \bar{J}_H \quad (27)$$

where

$$\begin{aligned}\bar{J}_H &= \sum_{i=0}^{\bar{N}_H-1} \|\bar{x}^{[M]}(k+i) - \bar{C}^\top y_{s,r}\|_{\bar{Q}_{s,H}}^2 + \|\Delta u_s^{[M]}(k+i)\|_{\bar{R}_{s,H}}^2 \\ &\quad + \gamma(\alpha(k+i) - 1)^2 + \|\bar{x}^{[M]}(k+\bar{N}_H) - \bar{C}^\top y_{s,r}\|_{\bar{P}_H}^2.\end{aligned}\quad (28)$$

γ is a positive scalar, $\bar{N}_H > N_\alpha$ is the adopted prediction horizon. The positive definite and symmetric weighting matrices $\bar{Q}_{s,H} \in \mathbb{R}^{(n+p_s) \times (n+p_s)}$, $\bar{R}_{s,H} \in \mathbb{R}^{m_s \times m_s}$ are free design parameters, while \bar{P}_H is computed as the solution to the Lyapunov equation

$$\bar{F}_{s,H}^\top \bar{P}_H \bar{F}_{s,H} - \bar{P}_H = -(\bar{Q}_{s,H} + \bar{K}_{s,H}^\top \bar{R}_{s,H} \bar{K}_{s,H}) \quad (29)$$

The optimization problem (27) is performed under the following constraints:

- (1) dynamics (24), constraint (21), and (26);
- (2) the state terminal constraint

$$\bar{x}^{[M]}(k+\bar{N}_H) \in \bar{\mathcal{X}}_F^s,$$

where $\bar{\mathcal{X}}_F^s \subseteq \bar{\mathcal{X}}_F$, the set $\bar{\mathcal{X}}_F^s$ is a positively invariant set for the nominal system of (24), i.e.,

$$z(k+1) = \bar{A}^{[M]}z(k) + \bar{B}_s^{[M]}\hat{u}(k), \quad (30)$$

that is controlled with the stabilizing control law $\hat{u}(k) = \bar{K}_{s,H}(z(k) - \bar{C}^\top y_{s,r})$ such that $\bar{F}_{s,H} \bar{\mathcal{X}}_F^s \subseteq \bar{\mathcal{X}}_F^s$ under constraint (26). The set $\bar{\mathcal{X}}_F^s$ is selected such that: for any $z(k) \in \bar{\mathcal{X}}_F^s$, the successive state under the above stabilizing control law satisfies $z(k+1) \in \bar{\mathcal{X}}_F^s$.

Let $\bar{\Delta u}_s^{[M]}(k:k+\bar{N}_H-1|k)$ be the optimal solution to optimization (27). The real input $u_s^{[M]}(k)$ at time instant k is given by $u_s^{[M]}(k) = u_s^{[M]}(k-1) + \bar{\Delta u}_s^{[M]}(k|k)$, also from (22) we can compute the value of $u_f^{[M]}(k)$. At this time instant, the state $\hat{x}^{[M]}(k+1|k)$ is available by applying $u^{[M]}(k) = (u_s^{[M]}(k), u_f^{[M]}(k))$ to (6).

In principle, the fast MPC problem described in the previous section, i.e., (13) with cost (15), can be used for computing the corrections of the control input in the fast time scale. We propose an improved algorithm in the following. Slightly different to (12) in (13), we use

$$\begin{cases} \Delta \hat{x}(h+i+1|h) = A \Delta \hat{x}(h+i|h) + B \Delta u(h+i|h) \\ \hat{y}(h+i|h) = \hat{y}(h+i-1|h) + C \Delta \hat{x}(h+i|h) \end{cases} \quad (31)$$

$h \in [kN, kN+N)$, to compensate for uncertainties.

Accordingly, at any fast time instant $h = kN + t$, letting $\bar{\Delta u}(h : (k+1)N - 1) = [\Delta u(h|h) \quad \dots \quad \Delta u((k+1)N - 1|h)] \in (\mathbb{R}^m)^{N-t}$, $\bar{\hat{x}} = (\hat{y}, \Delta \hat{x})$, and $\bar{y} = (\bar{y}^*, 0)$, the shrinking horizon MPC problem can be solved at the low level:

$$\min_{\bar{\Delta u}(h:(k+1)N-1)} \bar{J}_L \quad (32)$$

$$\bar{J}_L = \sum_{j=0}^{N-t-1} \|\bar{\hat{x}}(h+j|h) - \bar{y}(h)\|_{\bar{Q}}^2 + \|\Delta u(h+j|h)\|_{\bar{R}}^2 \quad (33)$$

where $\bar{Q} \in \mathbb{R}^{(n+p) \times (n+p)}$ is a positive-definite matrix. The optimization problem (32) is performed under the following constraints:

- (1) the dynamics (31);
- (2) the input constraint

$$\begin{aligned}u(kN-1) + \Delta u(kN|kN) &\in \mathcal{U}, \\ u(kN-1) + \sum_{i=0}^j \Delta u(h+i|h) &\in \hat{\mathcal{U}}^i, \quad \forall j = 1, \dots, N-t-1,\end{aligned}\quad (34)$$

where $i = h - kN$;

- (3) the state terminal constraint

$$\hat{x}(kN+N|h) = \hat{x}^{[M]}(k+1|k) \quad (35)$$

It is noted that constraints (34) and (35) can be rewritten following the line of (26), but the design steps are neglected for the sake of simplicity.

B. Summary of the Incremental D-MPC algorithm

To better clarify the requirements for implementing *Incremental D-MPC* and its difference with the D-MPC, the main steps for the on-line implementation are given in Algorithm 2.

Theorem 2: Under Assumptions 1–4, if the initial condition is such that $\hat{x}^{[M]}(0) = \hat{x}(0) = x(0)$ and N_α is reachable by Algorithm 2 such that (27) is feasible at $k = 0$, then the following results can be stated for the *Incremental D-MPC* algorithm under suitable conditions.

- (1) Provided that

$$(\bar{A}^{[M]})^{\bar{N}_H-1} E \mathcal{D} \subseteq \bar{\mathcal{X}}_F \ominus \bar{\mathcal{X}}_F^s \quad (36)$$

where $E = [\bar{C}_s^\top \quad I^\top]^\top$, and (18) is satisfied, then the feasibility can be guaranteed:

- for the high-level problem (27) at all slow time instant $k > 0$;
- for the low-level problem (32) at all fast time instant $h \geq 0$.

Algorithm 2 On-line implementation of *Incremental D-MPC*initialization with $N_\alpha = 1$ **while** for any integer $k \geq 0$ **do****h1)** compute the control $\Delta u_s^{[N]}(k|k)$ by solving the optimization problem (27) with (28) and update $\bar{x}^{[N]}(k+1|k)$ **if** (27) with (28) is infeasible **then**| $N_\alpha \leftarrow N_\alpha + 1$ and go back to step **h1)**, (see (21))**else**

| continue

end**h2)** calculate $u_f^{[N]}(k)$ from (22) with $u_s^{[N]}(k) = u_s^{[N]}(k-1) + \Delta u_s^{[N]}(k|k)$, apply the control $u^{[N]}(k) = (u_s^{[N]}(k), u_f^{[N]}(k))$ to (37) and update $x^{[N]}(k+1|k)$ **h3)** generate the open-loop output $\hat{y}^*(h)$ from (2) with $u(h) = u^{[N]}(\lfloor h/N \rfloor)$, for all $h \in [kN, kN+N)$ **for** $h \leftarrow kN$ **to** $kN+N-1$ **do****I1)** compute $\Delta u(h|h)$ using optimization problem (32) with (33) and apply $u(h) = u(h-1) + \Delta u(h|h)$ to (2)**I2)** update $x(h+1)$ and $y(h+1)$, set $\hat{x}(h+1) = x(h+1)$, $\hat{y}(h+1) = y(h+1)$ **end****h4)** $k \leftarrow k+1$ **end**(2) If the disturbance d is constant, then the asymptotic convergence of the closed-loop system can be ensured.

- The slow-time scale system (24) enjoys the convergence property, i.e., $\lim_{k \rightarrow +\infty} (\bar{x}^{[N]}(k), \Delta u_s^{[N]}(k)) = (\bar{C}^{-1} y_{s,r}, 0)$. Consequently, $\lim_{k \rightarrow +\infty} (x^{[N]}(k), u^{[N]}(k)) = (x_r, u_r)$.
- For the low-level problem (32), it holds that $\lim_{h \rightarrow +\infty} \Delta u(h) = 0$. Finally, $\lim_{h \rightarrow +\infty} (u(h), x(h), y(h)) = (u_r, x_r, y_r)$.

V. SIMULATION EXAMPLE

In this section, simulation results on a realistic BT system with comparisons in different domains are reported. For comparisons, in the nominal case, a multi-rate MPC in [29], two single-layer MPCs described in [33], a traditional decentralized PID controller, and a sliding mode controller (SMC) in [34] are used for comparison; while two single-layer robust MPC regulators designed according to [35] are also adopted in the perturbed case, two additional single-layer nonlinear MPC regulators in [36] and the sliding mode controller in [34] are introduced when applied to the nonlinear systems.

A. Description of the BT system and its linearized model

A 160 MW BT system in [37] is considered and its dynamic diagram is presented in Figure 3. The input variables applied to the boiler are the fuel flow q_f (kg/s) and feedwater flow q_w (kg/s), while the controlled variables of the boiler are drum pressure P (kg/cm²) and water level L (m). The control and controlled variables of the turbine are the steam control q_s (kg/s) and the electrical power output Q (MW). Typically, the goal of BT control is to regulate the electrical power to meet the load demand profile meanwhile to minimize the

variations of internal variables such as water level and drum pressure within their safe sets. Moreover, drum pressure must also be controlled properly in the operation range to respond to possible turbine speed changes caused by load demand variations. Many works have been addressed at this point that focus on deriving satisfactory closed-loop control performance of electrical power plants, see e.g. [38]–[42]. In this scenario, the control related to the output variables such as electrical power and drum pressure is a major issue that must be tackled properly to respond to frequent load demand variations, while the water level can be adjusted smoothly under its constraint with the possibility to follow its desired value. This makes it reasonable in this case to apply the proposed dual-level control algorithms. We adopt the nonlinear dynamic model of a BT system described in [37] as the case study. In the nonlinear system, the state variables are ρ, P, Q , where ρ is the fluid density (kg/cm³) that establishes a static mapping with the water level. The control variables are limited by $0 \leq q_f, q_w, q_s \leq 1$ and their rate constraints are also considered, i.e., $-0.007 \leq \dot{q}_f \leq 0.007$, $-2 \leq \dot{q}_s \leq 0.2$, $-0.05 \leq \dot{q}_w \leq 0.05$. The linearized model at an operation point $(\rho_r, P_r, Q_r) = (513.6, 129.6, 105.8)$, $(q_{w,r}, q_{f,r}, q_{s,r}) = (0.663, 0.505, 0.828)$ is considered as the controlled system, i.e.,

$$\begin{cases} \dot{x} = Ax + Bu \\ y = Cx, \end{cases} \quad (37)$$

where $C = I$, the state and output variables are $y = x = (\rho - \rho_r, P - P_r, Q - Q_r)$, while the input variables are $u = (q_w - q_{w,r}, q_f - q_{f,r}, q_s - q_{s,r})$. The unitary step response of (37) is presented in Figure 4, which displays that the system outputs are strongly coupled, and the dynamics is not strictly separable.

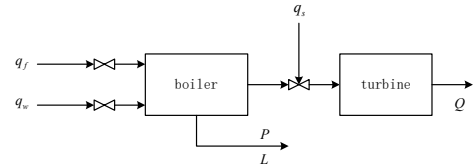


Fig. 3. Diagram of the BT dynamics.

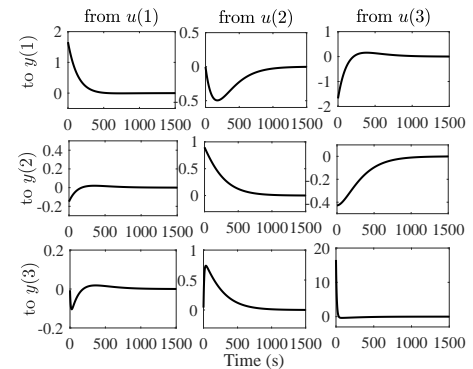


Fig. 4. Unitary impulse response of the BT dynamics.

B. Devising the D-MPC and Incremental D-MPC regulators

In order to implement the proposed dual-level control algorithms, the system's continuous-time model (37) has been sampled with $\Delta t = 1s$ to obtain the discrete-time counterpart in the fast time scale. The resulting system has been rewritten to derive model (1), where the input, state, and output variables associated with Σ_s to be controlled smoothly are chosen as $u_s = q_w - q_{w,r}$, $x_s = \rho - \rho_r$, and $y_s = x_s$ while the corresponding ones associated with Σ_f to be controlled in a prompt fashion are $u_f = (q_f - q_{f,r}, q_s - q_{s,r})$, $x_f = (P - P_r, Q - Q_r)$, and $y_f = x_f$. The resulting model has been re-sampled with $N = 20$ to obtain (6) and (19) to be used at the high level.

1) Design of the D-MPC regulator:

- The high-level MPC (8) with cost (9) has been implemented with $Q_H = I$ and $R_H = \text{diag}(2, 20, 20)$, and prediction horizon $N_H = 20$. The control gain matrix K_H is selected by solving an infinite horizon LQ problem. The terminal penalty P_H is computed according to (10). The terminal set has been chosen according to the algorithm described in [43].
- The low-level shrinking horizon MPC (13) with cost (14) has been designed with $Q = I$ and $R = \text{diag}(1, 1, 10)$.

2) Design of the Incremental D-MPC regulator:

- The high-level MPC (27) with cost (28) has been implemented with $N_\alpha = 2$ (see Algorithm 2), $\bar{Q}_H = I$ and $\bar{R}_H = \text{diag}(2, 20, 20)$, and prediction horizon $\bar{N}_H = 20$. The control gain matrix $\bar{K}_{s,H}$ is selected by solving the corresponding infinite horizon LQ problem. The terminal penalty is computed according to (10). Likewise, the terminal set has been chosen according to the algorithm described in [43].
- The low-level shrinking horizon MPC (32) with cost (33) has been designed with $\bar{Q} = I$ and $R = \text{diag}(1, 1, 10)$.

C. Simulation results: control of the linear nominal model

The proposed dual-level control algorithms have been applied to the linear BT system by solving an output reference tracking problem. The output set-point $y_r = (10, 2, -2)$ is initially considered; while at time $t = 400s$, the reference value has been reset according to the new load profile, i.e., $y_r = (5, 1, 4)$. The dual-level control algorithms have been implemented from null initial conditions. In the following, the simulation results have been reported including the comparisons with a multi-rate MPC in [29], two single-layer MPC regulators designed according to [33] working at different time scales, and a traditional decentralized PID controller.

1) *Design of the multirate MPC [29]:* Note that, due to the usage of finite impulse response representation, the model used for the multirate MPC must be strictly stable. However, the considered system in this paper has a pole on the unitary circle. In order to implement the multirate MPC successfully, a feedback compensator $u_s = ky_s + v$ has been used firstly, where v is defined as an auxiliary control variable, and the feedback gain k is chosen as $k = -0.005$.

For fair comparison, the design parameters Q_s and R_s have been selected coincident with the proposed MPC algorithms, i.e., $Q_s = \text{diag}\{1, 2, \dots, 2, 20, \dots, 20\}$, $R_s = 2$.

2) *Design of the single-layer MPCs [33]:* Two single-layer stabilizing MPCs are designed working in slow and fast time scales respectively. The sampling time period of the slow and fast single-layer MPCs have been chosen as $\Delta t = 20s, 1s$, and the prediction horizons of the slow and fast MPC has been set as N_H and N respectively. The design parameters Q and R have been set to the values same as the high-level of the D-MPC.

3) *Design of the decentralized PID controller:* The decentralized PIDs, one for each input/output pair, have been designed with all the selected tuning parameters listed in Table I.

TABLE I
TUNING PARAMETERS OF THE DECENTRALIZED PIDS

Control pair	Proportional (P)	Integral (I)	Derivative (D)
(u_s, y_s)	0.019	$2 \cdot 10^{-4}$	-0.07
$(u_f(1), y_f(1))$	0.24	0.006	-1
$(u_f(2), y_f(2))$	-0.035	$-4.6 \cdot 10^{-4}$	0.36

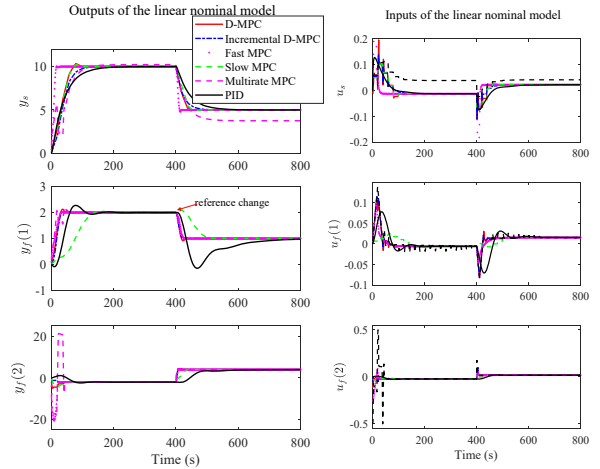


Fig. 5. Output and control variables of the controlled linear model.

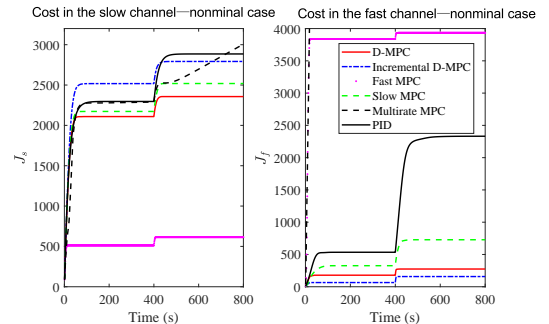


Fig. 6. The comparison of variations of cumulative square tracking errors among all the controllers in the nominal case: The proposed D-MPC and Incremental D-MPC have gained the smaller tracking costs of the fast (crucial) output y_f at the expense of larger ones of the slow (less crucial) output y_s .

4) *Simulation results:* All the comparative simulation experiments have been implemented within Yalmip toolbox installed in MATLAB environment, see [44], in a Laptop with Intel Core i9-9880H 2.30 GHz running Windows 10 operating system. The simulation results have been reported in Figures 5-6 and Figure 7. It can be seen in Figure 5 that, after an initial transient, inputs and outputs return to their nominal values, until the change of the reference occurs when the dual-level MPCs and single-layer MPCs properly react to bring the input and output variables to their new steady-state values, while the multirate MPC and decentralized PID controllers react more slowly to reference variations. Note that, the proposed dual-level algorithms exhibit better control performances than other approaches for the crucial pair (u_f, y_f) , while the fast MPC performs the best for the pair (u_s, y_s) , which in fact can be controlled smoothly in the considered problem. In Figure 6, the cumulative square tracking errors $J_s = \sum_{i=1}^{N_{\text{sim}}} \|y_s(i) - y_{s,r}\|^2$, and $J_f = \sum_{i=1}^{N_{\text{sim}}} \|y_f(i) - y_{f,r}\|^2$, along the simulation steps from $N_{\text{sim}} = 1$ to 800 are displayed for all the approaches, which show that, the proposed algorithms result smaller values of cost J_f than other approaches at the expense of a larger cost on J_s . The cost J_s with the fast MPC is the lowest but at the expense of a larger cost on J_f , i.e., a degradation of the control performance on (u_f, y_f) . Also, the cost J_f with the *Incremental* D-MPC is smaller than that with the D-MPC at the price of a slightly larger J_s . This reveals that the proposed D-MPC and *Incremental* D-MPC show strong points in imposing separable closed-loop dynamics, i.e., controlling the pair (u_f, y_f) promptly while regulating the less crucial pair (u_s, y_s) in a smoother fashion. Also, the *Incremental* D-MPC outperforms the D-MPC in this respect. As for computational resources, the average computational times of the proposed algorithms are smaller than that of the fast MPC in the nominal case, see Figure 7.

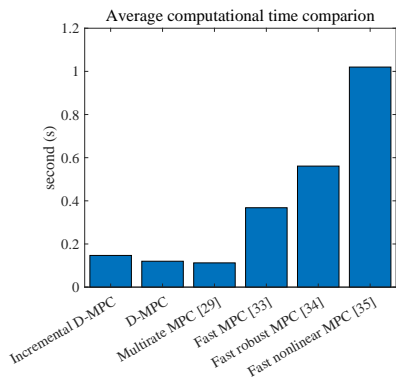


Fig. 7. Computational times comparison. The computational times of the proposed algorithms are smaller than that of the fast single-layer MPCs.

D. Simulation results: control of the linear model with uncertainties

To further verify the capability of the proposed algorithms in dealing with disturbances. A bounded unknown step-wise disturbance, i.e., $(-0.2, 0.05, -0.1) \leq d \leq (0.2, 0.1, 0.1)$, has been added to the controlled system, see Figure 8. In the

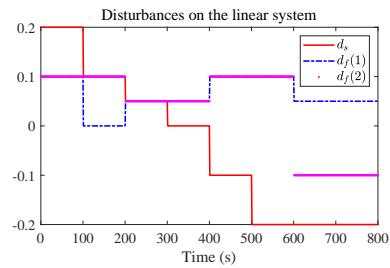


Fig. 8. Disturbances on the linear model.

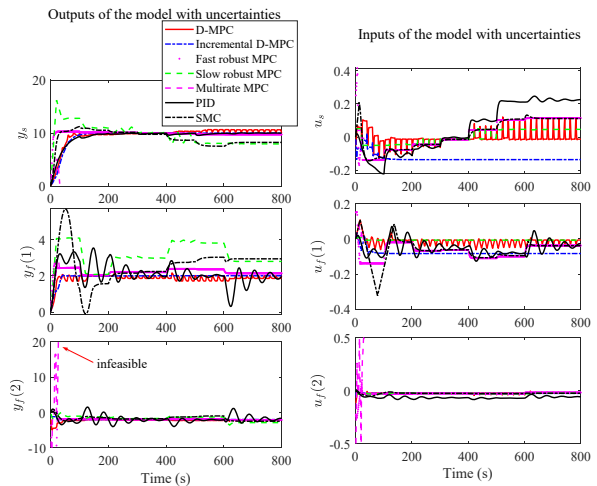


Fig. 9. Output and control variables of the controlled linear model with uncertainties.

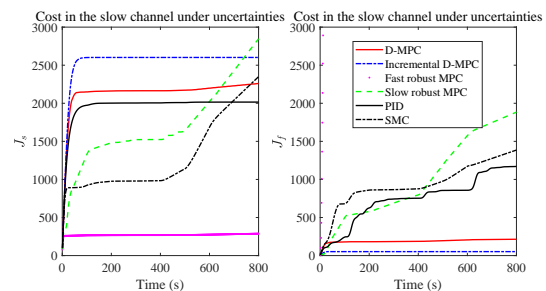


Fig. 10. The comparison of variations of cumulative square tracking errors among different controllers in the perturbed case: The proposed *Incremental* D-MPC is the only one that has realized offset-free control for both the fast and slow control channel. Note that, the *Incremental* D-MPC has gained the smallest tracking cost of the fast (crucial) output y_f at the expense of the largest one of the slow (less crucial) output y_s .

proposed controller, the control constraints have been properly tightened according to (18) and the terminal constraint has been computed according to [45]. For comparison, the multirate MPC [29], two single-layer robust MPC regulators in [35], the decentralized PID controller, and the sliding mode controller in [34] have been used. In the robust MPCs, the design parameters have been chosen similar to the nominal MPCs, except that the control constraints have been tightened according to the robust invariant set for real constraint satisfaction under perturbations and the optimization on the

initial nominal state has been considered, see [35]. In the sliding mode controller, all the parameters are fine tuned according to the design procedures in [34]. In the simulation tests, the output set-point regulation with $y_r = (10, 2, -2)$ has been considered. The corresponding simulation results are presented in Figures 9-10. The results show that, the proposed *Incremental* D-MPC can realize offset-free control for all the outputs, which is not yet realized by the D-MPC, the multirate MPC, the robust MPCs, the PIDs, and the SMC, since most of the cumulative costs are still increasing at the terminal simulation time, see Figure 10. Also, the multirate MPC is early terminated due to the in-feasibility issue caused by disturbances. It reveals that, the proposed *Incremental* D-MPC outperforms the multirate MPC, robust MPCs, and decentralized PIDs, and the SMC, especially in enforcing satisfactory control performance for the pair (u_f, y_f) , see again Figure 10. Also, the average computational times with the proposed algorithms are smaller than that of the fast robust MPC, see Figure 7.

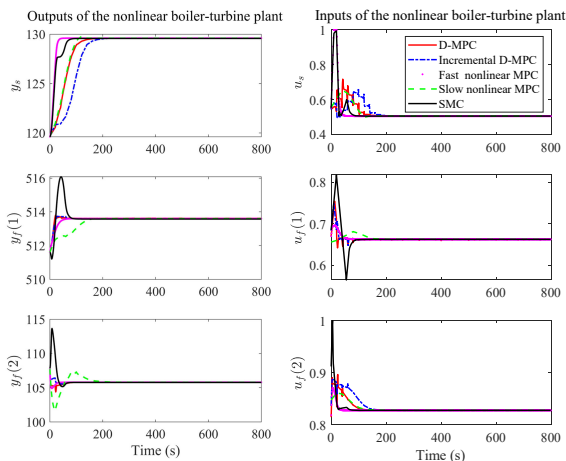


Fig. 11. Output and control variables of the nonlinear controlled boiler-turbine plant.

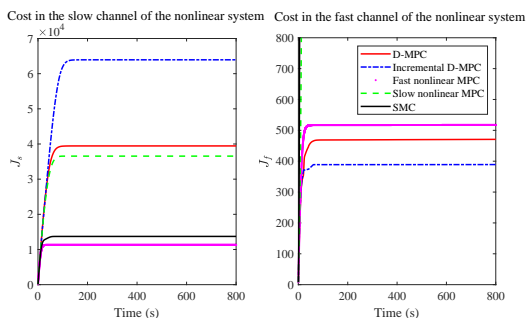


Fig. 12. The comparison of variations of cumulative square tracking errors of the nonlinear controlled systems: The proposed algorithms exhibit better control performance for the fast output y_f than the nonlinear MPCs. Note that, the proposed *Incremental* D-MPC has gained the smallest tracking cost of the fast (crucial) output y_f at the expense of the largest one of the slow (less crucial) output y_s .

E. Simulation results: application to the nonlinear system

Besides the verification of the developed theory in the nominal and perturbed cases, we have also applied the proposed algorithms to the original nonlinear systems, see [37]. Two single-layer nonlinear MPC regulators designed according to [36] and the SMC in [34] are used for fair comparison. In the nonlinear MPCs, the prediction horizons have been chosen as 20. The performance index adopted has been $J = \sum_{j=0}^{N_p-1} \|x(t+j) - x_r\|_{Q_H}^2 + \|u(t+j) - u_r\|_{R_H}^2 + \|x(t+N_p) - x_r\|_P^2$, where the terminal cost is added to guarantee stability and P is computed using the nominal linearized model. In the simulation test, the control goal has been to drive the state variable to the reference $x_r = (513.6, 129.6, 105.8)$ from the initial condition $x_0 = x_r + (10, 2, -2)$. The simulation results are reported in Figures 11-12. The results show that, the proposed *Incremental* D-MPC achieves the best control performance for (u_f, y_f) at the expense of the control performance degradation on (u_s, y_s) , see Figure 12. The fast nonlinear MPC and SMC perform better for (u_s, y_s) but worse than the proposed D-MPC and *Incremental* D-MPC in terms of that for (u_f, y_f) , hence it does not fulfill the control goal specified in this paper. Also, as shown in Figure 7, the average computational times of the proposed algorithms are much smaller than that of the fast nonlinear MPC.

F. Discussions

One can conclude from the above simulation tests that, the proposed algorithms, especially *Incremental* D-MPC, have fulfilled the control objective considered in this paper, i.e., generating satisfactory fast dynamics for the fast (crucial) pair (u_f, y_f) and smooth dynamics for the slow (less crucial) pair (u_s, y_s) , see Figures 6, 10, and 12. The former is enforced at the expense of the performance degradation of (u_s, y_s) . However, the control objective is not well met by the single-layer fast MPCs working in the basic time scale, see again Figures 6, 10, and 12, where differently, the control performances of the less crucial (u_s, y_s) are the best ones among all the controllers in the simulation tests. Note that, the proposed algorithms might not outperform single-layer MPCs when the overall control performance is a major concern, which is not in the scope of this paper. The computational times of the proposed algorithms are much smaller than that of the fast MPCs, due to the shrinking horizon strategy used in the basic time, see Figure 7.

Different from output-feedback controllers, the proposed approaches do not rely on an observer for estimating disturbances. The simulation results in Figures 9-10 reveals that the proposed approaches are robust to time-varying disturbances, and the *Incremental* D-MPC can realize offset-free control under unknown time-varying piece-wise disturbances. One limitation of the proposed algorithms lies in the boundedness assumption of the disturbances for the recursive feasibility guarantee of constrained control problems.

VI. CONCLUSIONS

In this paper, two dual-level MPC control algorithms have been proposed for linear multi-timescale systems with input

constraint. The proposed MPC algorithms rely on clear time separation, so allow to deal with control problems in different channels. In view of their main properties, the proposed algorithms are, based on the solution based on MPC with dual-level structure, suitable not only to cope with control of singularly perturbed systems but also to impose different closed-loop dynamical performance for systems with non-separable open-loop dynamics.

The recursive feasibility and convergence of the proposed D-MPC and *Incremental* D-MPC are proven under suitable assumptions. The effectiveness of the proposed algorithms is tested rigorously in different simulation scenarios, including numerous comparisons with different classic controllers. The simulation results show that both the proposed D-MPC and *Incremental* D-MPC are effective in imposing closed-loop separable dynamics and can deal with unknown bounded time-varying disturbances. Also, the latter can obtain offset-free control under unknown and rapidly varying step-wise disturbances without using a disturbance estimator.

Future work will consider extending the proposed framework to solving multi-rate control problems for systems with large time scales, possibly relies on a cloud-edge computing structure; and apply the proposed approaches to multi-agent control systems.

VII. ACKNOWLEDGMENT

The first author wishes to thank Prof. Riccardo Scattolini and Prof. Marcello Farina from Politecnico di Milano, for their fruitful discussions.

APPENDIX A

A. Proof of Proposition 1

According to PBH detectability rank test, the pair (A, C) is detectable if and only if $\text{rank}([\lambda I - A \quad C]) = n, \forall \lambda \in \mathbb{C}$ and $|\lambda| \geq 1$. An equivalent form to this condition is that $v = 0$ is the unique solution to the following linear equations

$$\begin{cases} Av = \lambda v \\ Cv = 0, \end{cases} \quad (38)$$

$\forall \lambda \in \mathbb{C}$ and $|\lambda| \geq 1$. From (38), $v = 0$ is the unique solution to $\lambda^{i-1}Av = \lambda^i v, Cv = 0, \forall i \in \mathbb{N}_+$, which is $A^i v = \lambda^i v, Cv = 0, \forall i \in \mathbb{N}_+$. In view of this, recalling that (A, C) is detectable, it holds that $v = 0$ is the only solution to

$$\begin{cases} A^{[M]}v = \mu v \\ Cv = 0, \end{cases}$$

where $\mu = \lambda^N$, which implies $(A^{[M]}, C)$ is observable for all the modes that their poles $|\lambda| \geq 1$. Hence, Proposition 1 holds. \square

B. Proof of Theorem 1

1) *Recursive feasibility of the D-MPC (i.e., high-level problem (8) and low-level problem (13))*: As the problem (8) is assumed to be feasible at time $k = 0$, with resorting to Mathematical Induction technique, one can prove the closed-loop recursive feasibility by verifying that if (8) is feasible at any time k , then

- (i) the low-level problem (13) is feasible at any fast time $h \in [kN, kN + N]$;
- (ii) also the high-level problem (8) is feasible at the subsequent slow time instant $k + 1$.

First, we show that condition (i) can be verified. To proceed, we assume that the high-level problem (8) is feasible at time k . Assume $\delta u(kN), \dots, \delta u(h|h), \dots, \delta u(kN + N - 1|h) \in \Delta \mathcal{U} \times \Delta \hat{\mathcal{U}}^{N-1}$ is a feasible solution at time $h \in [kN, kN + N - 2]$ and the terminal state constraint is verified. Letting $h = kN + j$, one has

$$\hat{x}^{[M]}(k+1|k) = \sum_{i=0}^{N-1} A^i Bu(kN+i|h) + A^N x(kN) + \sum_{i=0}^{j-1} A^{N-i-1} d(kN+i) \quad (39)$$

One can also write the predicted terminal state at time $h+1$, i.e.,

$$\hat{x}(kN+N|h+1) = \sum_{i=0}^{N-1} A^i Bu(kN+i|h+1) + A^N x(kN) + \sum_{i=0}^j A^{N-i-1} d(kN+i) \quad (40)$$

To ensure the recursive feasibility, it is required to enforce $\hat{x}(kN+N|h+1) = \hat{x}^{[M]}(k+1|k)$. By difference of (40) and (39), leads to

$$\sum_{i=j+1}^{N-1} A^{N-i-1} Bu(kN+i|h+1) = -A^{N-j-1} d(h) + \sum_{i=j+1}^{N-1} A^{N-i-1} Bu(kN+i|h) \in \Delta L^j \mathcal{U} \oplus L^{j+1} \hat{\mathcal{U}}^{j+1}, \quad (41)$$

in view of condition (18). Hence, the recursive feasibility at the low level follows.

As for (ii), first note that, one can compute the gap between the real state and the predicted one, i.e.,

$$x^{[M]}(k+1) - \hat{x}^{[M]}(k+1|k) = \tilde{d}^{[M]}(k) \quad (42)$$

Note that, $\hat{x}(kN+N|kN+N-1) = \hat{x}^{[M]}(k+1)$ and $x(kN+N) - \hat{x}(kN+N|kN+N-1) = d(kN+N-1)$. One promptly has

$$\tilde{d}^{[M]}(k) = d(kN+N-1).$$

Hence, one can also compute:

$$\hat{x}^{[M]}(k+N_H|k) - \hat{x}^{[M]}(k+N_H|k+1) = (A^{[M]})^{N_H-1} d(kN+N-1) \quad (43)$$

Assume that at any slow time instant k the optimal control sequence of (8) can be found, i.e., $\overrightarrow{u}^{[M],\sigma}(k : k+N_H-1|k) = (u^{[M],\sigma}(k|k), \dots, u^{[M],\sigma}(k+N_H-1|k))$ such that $x^{[M]}(k+N_H|k) \in \mathcal{X}_F^s$. Let the input sequence $\overrightarrow{u}^{[M],s}(k+1 : k+N_H|k+1) = (u^{[M],\sigma}(k+1|k), \dots, u^{[M],\sigma}(k+N_H-1|k), K_H(x^{[M]}(k+N_H|k) - x_r) + u_r)$ be a candidate choice at the next time instant $k+1$. As condition (17) is assumed, it holds that $\hat{x}(k+N_H|k+1) \in \mathcal{X}_F^s$. In view of this, $\hat{x}(k+N_H+1|k+1) \in \mathcal{X}_F^s$ can be verified in view of the definitions of K_H and \mathcal{X}_F^s . Hence, the recursive feasibility of (8) follows.

2) *Convergence of the closed-loop system*: We first prove the convergence of the high-level problem (8). As the disturbance $d = 0$, it holds that $\hat{x} = x, \hat{y} = y$. Denote by $J_H^{\sigma}(x^{[M]}(k))$ the optimal cost associated with $\overrightarrow{u}^{[M],\sigma}(k : k+N_H-1|k)$ at time

k and by $J_H^s(x^{[M]}(k+1|k))$ the suboptimal cost associated with $\vec{u}^{[M],s}(k+1:k+N_H|k+1)$ at time $k+1$. It is possible to write

$$\begin{aligned} & J_H^s(x^{[M]}(k+1|k)) - J_H^o(x^{[M]}(k)) = \\ & = -(\|y^{[M]}(k) - y_r\|_{Q_H}^2 + \|u^{[M],o}(k|k) - u_r\|_{R_H}^2) + \\ & \quad \|y^{[M]}(k+N|k) - y_r\|_{Q_H}^2 + \|K_H(x^{[M]}(k+N_H|k) - x_r)\|_{R_H}^2 + \\ & \quad \|F_H(x^{[M]}(k+N|k) - x_r)\|_{P_H}^2 - \|x^{[M]}(k+N|k) - x_r\|_{P_H}^2 \\ & = -(\|y^{[M]}(k) - y_r\|_{Q_H}^2 + \|u^{[M],o}(k|k) - u_r\|_{R_H}^2) \\ & \quad + \|x^{[M]}(k+N|k) - x_r\|_{F_H^\top P_H F_H - P_H + C^\top Q_H C + K_H^\top R_H K_H}^2 \end{aligned} \quad (44)$$

In view of (10) and from (44), one has

$$\begin{aligned} & J_H^s(x^{[M]}(k+1|k)) - J_H^o(x^{[M]}(k)) = \\ & -(\|y^{[M]}(k) - y_r\|_{Q_H}^2 + \|u^{[M],o}(k|k) - u_r\|_{R_H}^2). \end{aligned}$$

Recalling the fact that $J_H^o(x^{[M]}(k+1|k)) \leq J_H^s(x^{[M]}(k+1|k))$, then

$$\begin{aligned} & J_H^o(x^{[M]}(k+1|k)) - J_H^o(x^{[M]}(k)) \leq \\ & -(\|y^{[M]}(k) - y_r\|_{Q_H}^2 + \|u^{[M],o}(k|k) - u_r\|_{R_H}^2), \end{aligned} \quad (45)$$

which implies that $J_H^o(x^{[M]}(k+1|k)) - J_H^o(x^{[M]}(k))$ converges to zero. Moreover, from (45), one has $J_H^o(x^{[M]}(k)) - J_H^o(x^{[M]}(k+1|k)) \geq \|y^{[M]}(k) - y_r\|_{Q_H}^2 + \|u^{[M],o}(k|k) - u_r\|_{R_H}^2$, then $\|y^{[M]}(k) - y_r\|_{Q_H}^2 + \|u^{[M],o}(k|k) - u_r\|_{R_H}^2 \rightarrow 0$. Recalling the definitions of Q_H and R_H , one has $\lim_{k \rightarrow +\infty} y^{[M]}(k) = y_r$ and $\lim_{k \rightarrow +\infty} u^{[M]}(k) = u_r$. In view of Proposition 1, consequently $\lim_{k \rightarrow +\infty} x^{[M]}(k) = x_r$.

As for the convergence of the low-level problem (13), assume that the high-level system variables have reached their reference values, i.e., $u^{[M]}(k) \equiv u_r$, $x^{[M]}(k) \equiv x_r$, $y^{[M]}(k) \equiv y_r$. Define $\delta x(k) = x(kN) - x_r$ and $\delta y(k) = y(kN) - y_r$. Along the same line in [30], in view of dynamics (12) at time instant $h = kN$, the low-level dynamics at the slow time scale is defined

$$\begin{cases} \delta x(k+1) = A^N \delta x(k) + w(k) \\ \delta y(k) = C \delta x(k), \end{cases} \quad (46)$$

where $w(k) = \sum_{j=0}^{N-1} A^{N-j-1} B \delta u(kN+j)$. Since $\delta x(k) = 0, \forall k \geq 0$ (due to (16)), it holds that $w(k) = 0$. In view of the cost function at the low level, the null sequence $\vec{\delta u}(h : (k+1)N-1) = 0$ solves the problem (8), which implies that $\lim_{h \rightarrow +\infty} \delta u(h) = 0$ and $\lim_{h \rightarrow +\infty} u(h) = u_r$. Finally, $\lim_{h \rightarrow +\infty} y(h) = y_r$ and $\lim_{h \rightarrow +\infty} x(h) = x_r$. \square

C. Proof of proposition 2

According to PBH stabilizability rank test, the pair $(\bar{A}^{[M]}, \bar{B}_s^{[M]})$ is stabilizable if and only if $\text{rank}([\lambda I - \bar{A}^{[M]} \quad \bar{B}_s^{[M]}]) = n + p_s$, for $\lambda \in \mathbb{C}$ and $|\lambda| \geq 1$. An equivalent form to this condition is that $v = 0$ is the unique solution to the following linear equations

$$\begin{cases} (\bar{A}^{[M]})^\top v = \lambda v \\ (\bar{B}_s^{[M]})^\top v = 0, \end{cases} \quad (47)$$

where $\lambda \in \mathbb{C}$ and $|\lambda| \geq 1$.

In view of (24), it is possible to write (47) in the form

$$\begin{bmatrix} I - \lambda I & 0 \\ \tilde{C}_s \tilde{A}^{[M]} & \tilde{A}^{[M]} - \lambda I \\ \tilde{C}_s \tilde{B}_s^{[M]} & \tilde{B}_s^{[M]} \end{bmatrix}^\top v = 0 \quad (48)$$

Since $\tilde{A}^{[M]}$ is stabilizable by Assumption 4, it is obvious to see that for $|\lambda| > 1$, $v = 0$ is the unique solution to (48).

For $\lambda = 1$, $v = 0$ is the unique solution to (48) if and only if

$$\text{rank} \begin{pmatrix} \tilde{C}_s \tilde{A}^{[M]} & \tilde{A}^{[M]} - I \\ \tilde{C}_s \tilde{B}_s^{[M]} & \tilde{B}_s^{[M]} \end{pmatrix}^\top = n + p_s.$$

As for $\lambda = -1$, $v = 0$ is the unique solution to (48) if and only if

$$\text{rank} \begin{pmatrix} 2I & 0 \\ \tilde{C}_s \tilde{A}^{[M]} & \tilde{A}^{[M]} + I \\ \tilde{C}_s \tilde{B}_s^{[M]} & \tilde{B}_s^{[M]} \end{pmatrix}^\top = n + p_s. \quad \square$$

D. Proof of Theorem 2

1) *Recursive feasibility of the Incremental D-MPC (i.e., high-level problem (27) and low-level problem (32))*: As N_α is assumed to be reachable by Algorithm 2 such that (27) is feasible at time $k=0$, along the same line of Section A-B, we first prove the recursive feasibility for problem (32) in the fast time scale. To this end, we assume (32) is feasible at a time instant $h \in [kN, kN+N)$, i.e., one can find the candidate control sequence $\Delta u(kN), \dots, \Delta u(h|h), \dots, \Delta u(kN+N-1|h)$ such that $\delta u(kN), \dots, \delta u(h|h), \dots, \delta u(kN+N-1|h) \in \Delta \mathcal{U} \times \Delta \mathcal{Q}^{N-1}$ and the terminal state constraint is verified. Along the same line with Appendix A-B, one requires condition (41), which is verified in view of (18). Hence, the recursive feasibility at the low level follows.

As for a sketch of the proof of the feasibility at the high level, first note that, one can compute:

$$\begin{aligned} \Delta x^{[M]}(k+1) - \Delta \hat{x}^{[M]}(k+j|k) &= x^{[M]}(k+1) - \hat{x}^{[M]}(k+1|k) \\ &= d(kN+N-1) \end{aligned} \quad (49)$$

Recalling that $\bar{x}^{[M]} = (y_s^{[M]}, \Delta x^{[M]})$, one can also compute:

$$\bar{x}^{[M]}(k+\bar{N}_H|k) - \bar{x}^{[M]}(k+\bar{N}_H|k+1) = (\bar{A}^{[M]})^{\bar{N}_H-1} E d(kN+N-1) \quad (50)$$

Let assume at time k that the optimal control sequence (8) is found, i.e., $\vec{u}^{[M],o}(k:k+\bar{N}_H-1|k) = (\Delta u_s^{[M],o}(k|k), \dots, \Delta u_s^{[M],o}(k+\bar{N}_H-1|k))$ such that constraint (26) is fulfilled and $\bar{x}^{[M]}(k+\bar{N}_H|k) \in \mathcal{X}_F^s$. Noting the fact that $\bar{N}_H \geq N_\alpha$, one has $\alpha(k+\bar{N}_H) = 1 \forall k \geq 0$. Let $\Delta u_s^{[M],s}(k+1:k+\bar{N}_H+1|k+1) = (\Delta u_s^{[M],o}(k+1|k), \dots, \Delta u_s^{[M],o}(k+\bar{N}_H-1|k), \bar{K}_{s,H}(\bar{x}^{[M]}(k+\bar{N}_H|k) - \bar{C}^\top y_{s,r}))$ be the candidate input sequence at the next time instant $k+1$. As condition (36) is assumed, it holds that $\bar{x}(k+\bar{N}_H|k+1) \in \mathcal{X}_F^s$. In view of this, $\bar{x}(k+\bar{N}_H+1|k+1) \in \mathcal{X}_F^s$ can be verified in view of the definitions of $\bar{K}_{s,H}$ and \mathcal{X}_F^s . Hence, the recursive feasibility of (27) follows.

2) *Convergence of the Incremental D-MPC*: In view of (21) and recalling the feasibility result of (27) under d being constant, along the same line of Section A-B, one can compute

$$\begin{aligned} & \bar{J}_H^o(\bar{x}^{[M]}(k+1|k)) - \bar{J}_H^o(\bar{x}^{[M]}(k)) \leq \\ & -(\|\bar{x}_s^{[M]}(k) - \bar{C}^\top y_{s,r}\|_{Q_{s,H}}^2 + \|\Delta u_s^{[M],o}(k|k)\|_{\bar{K}_{s,H}}^2) \end{aligned} \quad (51)$$

where \bar{J}_H^o is the optimal cost. (51) implies that $\bar{J}_H^o(\bar{x}^{[M]}(k+1|k)) - \bar{J}_H^o(\bar{x}^{[M]}(k))$ converges to zero. Consequently, it holds

that $\|\bar{x}_s^{[N]}(k) - \bar{C}^\top y_{s,r}\|_{\bar{Q}_H}^2 + \|\Delta u_s^{[N],o}(k|k)\|_{\bar{R}_H}^2 \rightarrow 0$ as well. Recalling the definitions of \bar{Q}_H and \bar{R}_H , it holds that $\lim_{k \rightarrow +\infty} \bar{x}_s^{[N]}(k) = \bar{C}^\top y_{s,r}$ and $\lim_{k \rightarrow +\infty} \Delta u_s^{[N]}(k) = 0$. Consequently, one has $\lim_{k \rightarrow +\infty} y_s^{[N]}(k) = y_r$, $\lim_{k \rightarrow +\infty} u_s^{[N]}(k) = \text{const}$. In view of Proposition 1, it promptly follows that, $\lim_{k \rightarrow +\infty} x^{[N]}(k) = x_r$, $\lim_{k \rightarrow +\infty} u_s^{[N]}(k) = u_{s,r}$. The arguments for the results $\lim_{h \rightarrow +\infty} \Delta u(h) = 0$, $\lim_{h \rightarrow +\infty} y(h) = y_r$ are similar to Section A-B. Consequently, one has $\lim_{h \rightarrow +\infty} x(h) = x_r$, and $\lim_{h \rightarrow +\infty} u(h) = u_r$. \square

REFERENCES

- [1] D. Naidu, "Singular perturbations and time scales in control theory and applications: an overview," *Dynamics of Continuous Discrete and Impulsive Systems Series B*, vol. 9, pp. 233–278, 2002.
- [2] P. Kokotović, H. K. Khalil, and J. O'reilly, *Singular perturbation methods in control: analysis and design*. SIAM, 1999.
- [3] E. Mishchenko, *Asymptotic methods in singularly perturbed systems*. Consultants Bureau, 1994.
- [4] D. Naidu, *Singular perturbation methodology in control systems*. IET, 1988, no. 34.
- [5] J. Rodriguez-Vasquez, R. Perez, J. Moriano, and J. González, "Advanced control system of the steam pressure in a fire-tube boiler," *IFAC Proceedings Volumes*, vol. 41, no. 2, pp. 11 028–11 033, 2008.
- [6] A. Liniger, A. Domahidi, and M. Morari, "Optimization-based autonomous racing of 1: 43 scale rc cars," *Optimal Control Applications and Methods*, vol. 36, no. 5, pp. 628–647, 2015.
- [7] R. Verschuere, S. De Bruyne, M. Zanon, J. V. Frasch, and M. Diehl, "Towards time-optimal race car driving using nonlinear MPC in real-time," in *53rd IEEE conference on decision and control*. IEEE, 2014, pp. 2505–2510.
- [8] B. Paden, M. Čáp, S. Z. Yong, D. Yershov, and E. Frazzoli, "A survey of motion planning and control techniques for self-driving urban vehicles," *IEEE Transactions on intelligent vehicles*, vol. 1, no. 1, pp. 33–55, 2016.
- [9] M. G. Forbes, R. Patwardhan, H. Hamadah, and R. Gopaluni, "Model predictive control in industry: Challenges and opportunities," *IFAC-PapersOnLine*, vol. 48, no. 8, pp. 531–538, 2015.
- [10] S. J. Qin and T. A. Badgwell, "A survey of industrial model predictive control technology," *Control Engineering Practice*, vol. 11, no. 7, pp. 733–764, 2003.
- [11] M. Li, P. Zhou, H. Wang, and T. Chai, "Nonlinear multiobjective MPC-based optimal operation of a high consistency refining system in papermaking," *IEEE Transactions on Systems, Man, and Cybernetics: Systems*, no. 99, pp. 1–8, 2017.
- [12] Q. Jin, S. Wu, and R. Zhang, "Improved constrained model predictive tracking control for networked coke furnace systems over uncertainty and communication loss," *IEEE Transactions on Systems, Man, and Cybernetics: Systems*, no. 99, pp. 1–8, 2018.
- [13] S. Roshany-Yamchi, M. Cychowski, R. R. Negenborn, B. De Schutter, K. Delaney, and J. Connell, "Kalman filter-based distributed predictive control of large-scale multi-rate systems: Application to power networks," *IEEE Transactions on Control Systems Technology*, vol. 21, no. 1, pp. 27–39, 2013.
- [14] Y. Zhou, H. Hu, Y. Liu, S. Lin, and Z. Ding, "A real-time and fully distributed approach to motion planning for multirobot systems," *IEEE Transactions on Systems, Man, and Cybernetics: Systems*, vol. 49, no. 12, pp. 2636–2650, 2019.
- [15] F. Santoso, M. A. Garratt, S. G. Anavatti, and I. Petersen, "Robust hybrid nonlinear control systems for the dynamics of a quadcopter drone," *IEEE Transactions on Systems, Man, and Cybernetics: Systems*, no. 99, pp. 1–13, 2018.
- [16] Z. Zhou, B. De Schutter, S. Lin, and Y. Xi, "Two-level hierarchical model-based predictive control for large-scale urban traffic networks," *IEEE Transactions on Control Systems Technology*, vol. 25, no. 2, pp. 496–508, 2017.
- [17] Q. Fang, J. Wang, Q. Gong, and M. Song, "Thermal-aware energy management of an hpc data center via two-time-scale control," *IEEE Transactions on Industrial Informatics*, vol. 13, no. 5, pp. 2260–2269, 2017.
- [18] X. Chen, M. Heidarinejad, J. Liu, and P. Christofides, "Composite fast-slow MPC design for nonlinear singularly perturbed systems," *AICHE Journal*, vol. 58, no. 6, pp. 1802–1811, 2012.
- [19] X. Chen, M. Heidarinejad, J. Liu, D. de la Peña, and P. Christofides, "Model predictive control of nonlinear singularly perturbed systems: Application to a large-scale process network," *Journal of Process Control*, vol. 21, no. 9, pp. 1296–1305, 2011.
- [20] M. Ellis, M. Heidarinejad, and P. D. Christofides, "Economic model predictive control of nonlinear singularly perturbed systems," *Journal of Process Control*, vol. 23, no. 5, pp. 743–754, 2013.
- [21] L. Ma, C. Cai, and X. Ma, "Slow sampling control of singularly perturbed systems subject to actuator saturation and l2 disturbance," *Asian Journal of Control*, vol. 19, no. 4, pp. 1316–1328, 2017.
- [22] Y. Miao, L. Ma, X. Ma, and L. Zhou, "Fast sampling control of singularly perturbed systems with actuator saturation and disturbance," *Mathematical Problems in Engineering*, vol. 2015, 2015.
- [23] M. Wogrin and L. Glielmo, "An MPC scheme with guaranteed stability for linear singularly perturbed systems," in *Decision and Control (CDC), 2010 49th IEEE Conference on*. IEEE, 2010, pp. 5289–5295.
- [24] J. Niu, J. Zhao, Z. Xu, and J. Qian, "A two-time scale decentralized model predictive controller based on input and output model," *Journal of Analytical Methods in Chemistry*, vol. 2009, 2009.
- [25] M. Brdys, M. Grochowski, T. Gminski, K. Konarczak, and M. Drewa, "Hierarchical predictive control of integrated wastewater treatment systems," *Control Engineering Practice*, vol. 16, no. 6, pp. 751–767, 2008.
- [26] M. Ohshima, I. Hashimoto, H. Ohno, M. Takeda, T. Yoneyama, and F. Gotoh, "Multirate multivariable model predictive control and its application to a polymerization reactor," *International Journal of Control*, vol. 59, no. 3, pp. 731–742, 1994.
- [27] E. Van Henten and J. Bontsema, "Time-scale decomposition of an optimal control problem in greenhouse climate management," *Control Engineering Practice*, vol. 17, no. 1, pp. 88–96, 2009.
- [28] P. Sanila and J. Jacob, "Simultaneous tracking and vibration control of flexible joint manipulator using laguerre network based composite fast-slow mpc," in *Signal Processing, Informatics, Communication and Energy Systems (SPICES), 2015 IEEE International Conference on*. IEEE, 2015, pp. 1–6.
- [29] X. Zhang, M. Farina, S. Spinelli, and R. Scattolini, "A multi-rate model predictive control algorithm for systems with fast-slow dynamics," *IET Control Theory & Applications*, September 2018.
- [30] B. Picasso, X. Zhang, and R. Scattolini, "Hierarchical model predictive control of independent systems with joint constraints," *Automatica*, vol. 74, pp. 99–106, 2016.
- [31] B. Picasso, D. De Vito, R. Scattolini, and P. Colaneri, "An MPC approach to the design of two-layer hierarchical control systems," *Automatica*, vol. 46, no. 5, pp. 823–831, 2010.
- [32] G. Betti, M. Farina, and R. Scattolini, "A robust MPC algorithm for offset-free tracking of constant reference signals," *IEEE Transactions on Automatic Control*, vol. 58, no. 9, pp. 2394–2400, 2013.
- [33] J. B. Rawlings, D. Q. Mayne, and M. Diehl, *Model predictive control: theory, computation, and design*. Nob Hill Publishing Madison, WI, 2017, vol. 2.
- [34] Z. Guo, Q. Ma, J. Guo, B. Zhao, and J. Zhou, "Performance-involved coupling effect-triggered scheme for robust attitude control of hrv," *IEEE/ASME Transactions on Mechatronics*, vol. PP, no. 99, pp. 1–1, 2020.
- [35] I. Kiaei and S. Lotfifard, "Tube-based model predictive control of energy storage systems for enhancing transient stability of power systems," *IEEE Transactions on Smart Grid*, vol. 9, no. 6, pp. 6438–6447, 2017.
- [36] Z. Lu, W. Lin, G. Feng, and F. Wan, "A study of nonlinear control schemes for a boiler-turbine unit," *IFAC Proceedings Volumes*, vol. 43, no. 14, pp. 1368–1373, 2010.
- [37] K. Åström and R. Bell, "Dynamic models for boiler-turbine alternator units: Data logs and parameter estimation for a 160 MW unit," *Technical Reports*, 1987.
- [38] P. Chen, "Multi-objective control of nonlinear boiler-turbine dynamics with actuator magnitude and rate constraints," *ISA transactions*, vol. 52, no. 1, pp. 115–128, 2013.
- [39] X. Liu, P. Guan, and C. Chan, "Nonlinear multivariable power plant coordinate control by constrained predictive scheme," *IEEE Transactions on Control Systems Technology*, vol. 18, no. 5, pp. 1116–1125, 2009.
- [40] X. Liu and X. Kong, "Nonlinear fuzzy model predictive iterative learning control for drum-type boiler-turbine system," *Journal of Process Control*, vol. 23, no. 8, pp. 1023–1040, 2013.
- [41] X. Liu and J. Cui, "Economic model predictive control of boiler-turbine system," *Journal of Process Control*, vol. 66, pp. 59–67, 2018.
- [42] —, "Fuzzy economic model predictive control for thermal power plant," *IET Control Theory & Applications*, vol. 13, no. 8, pp. 1113–1120, 2019.

- [43] X. Hu and W. Chen, "Model predictive control: terminal region and terminal weighting matrix," *Proceedings of the Institution of Mechanical Engineers, Part I: Journal of Systems and Control Engineering*, vol. 222, no. 2, pp. 69–79, 2008.
- [44] J. Löfberg, "Yalmip : A toolbox for modeling and optimization in matlab," in *In Proceedings of the CACSD Conference*, Taipei, Taiwan, 2004.
- [45] D. Limone, T. Alamo, and E. Camacho, "Input-to-state stable MPC for constrained discrete-time nonlinear systems with bounded additive uncertainties," in *Proceedings of the 41st IEEE Conference on Decision and Control, 2002*, vol. 4. IEEE, 2002, pp. 4619–4624.